Structural and Multidisciplinary Optimization (2019) 59:279–289
https://doi.org/10.1007/s00158-018-2065-5

INDUSTRIAL APPLICATION

Multi-objective optimization of electric multiple unit wheel profile from wheel flange wear viewpoint

Dabin Cui[1,2] · Ruichen Wang[3] · Paul Allen[3] · Boyang An[2] · Li Li[1] · Zefeng Wen[4]

Received: 12 April 2018 / Revised: 7 July 2018 / Accepted: 7 August 2018 / Published online: 3 September 2018

Abstract

The CRH1 train is one of the main commuter trains in China which is mostly operating on typical and high-speed lines. Previously, a high-speed car wheel profile was used on the CRH1 train, but it does not match well with the train suspension parameters and also causes the instability of the train on tangent track and large curved track. Therefore, a new profile was designed as the replacement of the old one for the CRH1 train. However, the use of the new profile results in the serious wheel flange and rail gauge corner wear but it can provide better stability compared to the old profile. This paper first presents the evaluation of using the two profiles, and then a development of the wheel profile is objected in terms of both currently used profiles, which is not only to minimize the flange wear and also take the vehicle dynamic behavior into consideration. A multi-objective optimization method was, therefore, to propose for the minimization of the lateral force and the stability of wheelsets. The requirements of the wheel profile geometry are investigated through proposed optimization method. Finally, the profile satisfied the safety requirements of the vehicle has been provided by using the particle swarm optimization method. Furthermore, the evaluation of vehicle dynamic has been performed by using Multi-Body Simulation Software. The entire design process has been completed in a closed-loop procedure programed in MATLAB. The findings show that the developed profile after the optimization procedure is fairly acceptable for the requirements of the wheel-rail interface and dynamic behavior of CRH1 train.

Keywords Multi-objective optimization · Flange wear · Wheel profile design · Vehicle dynamic behavior

1 Introduction

Trains running mile after mile put high demands on their wheels. Each year, the cost of maintenance and replacement of wheel/rail wear in current rails is as high cost as several billion RMB (¥) in China (Jin and Shen 2001). With a large number of electric multiple unit (EMU) train come into service, the quality of railway in service have been greatly improved in the last decade. Meanwhile, wheel and rail wear has attracted much more attention by railway researchers and engineers. It can be assumed that the demand of high-speed wheels is more than 20,000 per year (Zhang and Gu 2009). If the wheel cannot suitably match the rail, the extra wear would be taken, and the normal operation could even be affected. The additional wear can be produced by the use of the un-matched wheel-rail profiles and exert negative influence on the operation of the train.

The wheel profile optimization is a long-standing research topic on railway. Since the nineteenth century, there has been a basic understanding of wheel shape and its self-steering principle (Wickens 1998). Based on many years' experience of research and operation (Heumann 1934; Yang 1978a, b; Liu 2000; Sato 2000), the wheel profile has been changed from conical wheel profile to worn wheel profile, and therefore the wear of the wheel/rail was significantly reduced to an acceptable level. At present, most of wheel profiles used in EMU trains have followed this design concept. Nowadays, a plenty of design concepts and methods were presented for the

Responsible editor: Somanath Nagendra

✉ Dabin Cui
cdb1645@163.com

[1] School of Mechanical Engineering, Southwest Jiaotong University, Chengdu 610031, China

[2] Key Laboratory of High-speed Railway Engineering, Ministry of Education, Chengdu 610031, China

[3] Institute of railway research, University of Huddersfield, Huddersfield HD1 3DH, UK

[4] State Key Laboratory of Traction Power, Southwest Jiaotong University, Chengdu 610031, China

optimization of the wheel profiles because of the rapid development of the numerical optimization techniques. Haque et al. (1989) developed a new wheel profile design method to balance the stability on a straight line with the performance on curved line. Yamada and Sasaki et al. (Sato 2005) designed a CS profile in terms of the measured rail profiles. Wu (Wu 2000) proposed a concept of wheel profile design to systemically evaluate the compatibility of the wheel and rail profile based on the vehicle characteristics and the operating condition. Zhang et al. (Zhang et al. 2008) applied the partial rail profile expansion method to design wheel profile with Chinese 60-kg/m rail. Shevtsov et al. (2005) (Markine et al. 2007) presented a numerical optimization technique based on rolling radius difference (RRD) of wheelset to design the wheel profile. Shen et al. (2003, 2005) (Shen and Zhong 2010) developed a method, so-called inverse methodology, for the design of railway wheel profile involving contact angle and rail profile information. A similar approach was proposed by Jahed et al. (2008) wherein the RRD function was also used for the design of railway wheel profiles. Polach (2011) proposed a new wheel tread profile design method which was considering the target conicity and wide tread wear spreading. Ignesti et al. (2013) presented two profiles designed with the objective of improving stability behavior and minimizing the wear. Cui et al. (Cui et al. 2011; Cui et al. 2015) used a wheel profile design method for EMU train with the considerations of the suspension parameters and wear performance.

The abovementioned studies have summarized some fundamental studies and field experience on the development of wheel profile, and clear development of typical wheel profile issues are introduced, including the reasons why a wheel profile is the best alternative solution to satisfy the requirements of different operating conditions. However, most of the current wheel profile optimization methods are aimed at vehicle dynamic behavior on tangent track. Only a few articles considering flange wear are simple verification of the wheel flange wear after optimization, and the optimization design goal of combining running behavior on tangent line and flange wear has not been given directly.

According to the rapid development of the EMU trains in the last two decades, the increasing vehicle speed and carrying capability bring new challenges for the design of wheel profiles. The CRH1 train is one of the main commuter trains in China. The CRH1 trains are running on the majority of the normal-speed lines and high-speed lines. The quality of high-speed lines is much better than the normal-speed lines. The LMA profile is a wheel profile which is used on high-speed locomotive and car in China, but this wheel profile is not able to achieve the requirements of the suspension of the CRH1 train, and the serious lateral vibration occurs when it operates at high speed. The alternative wheel profile, LMD, was designed to improve the stability of the wheelset but it can cause the wear on the wheel flange/rail gauge corner. The unexpected wear can definitely increase the cost of wheel/rail maintenance and also has impacts on the vehicle dynamics in some sections.

In order to design an optimal wheel profile for the CRH1 train, the performance of LMA and LMD was comparatively evaluated, including the wheel/rail contact geometry characters, the wheel/rail contact mechanical property, and the vehicle dynamic behavior. Then, a multi-objective optimization method was developed to reduce wear of wheel/rail and improve stability of wheelset. Finally, a new wheel profile was proposed in terms of the optimization method and the behavior of the CRH1 train was discussed.

2 Performances of LMA and LMD

LMA and LMD are the two typical wheel profiles which are used for CRH1 trains. Attempting to obtain a better profile, the performance of LMA and LMD was carefully analyzed to expose their advantages. In the analysis, the Chinese 60-kg/m rail (CN60) with 1353-mm rail gauge and 1/40 rail cant was used. The back to back distance of the wheel is set to 1435 mm.

The design of CRH1 bogie is shown in Fig. 1 and the main parameters of the CRH1 train are listed in Table 1. In the optimization progress, only a trailer car is selected and applied; the evaluation is assumed to ignore the influence of train formation.

First of all, it is worthy to discuss the geometry of the wheel profiles. LMA wheel profile was in use prior to the LMD profile designed. The geometry of the two proposed wheel profiles are shown in Fig. 2. They were designed to have the same flange shape and rim width, and obvious difference can be found in the region of wheel tread and flange root. The slope of LMD is

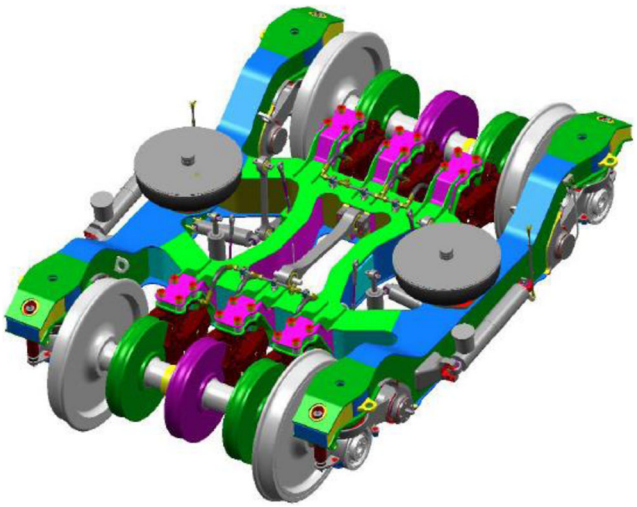

Fig. 1 The bogie of CRH1 train

Table 1 Main parameters of the CRH1 train

Mass of the coach	40,560	kg
Mass of the bogie	1432	kg
Mass of the wheelset	1621	kg
Primary suspension, longitudinal stiffness	2.4 E7	N/m
Primary suspension, lateral stiffness	6.0 E6	N/m
Primary suspension, vertical stiffness	7.965 E5	N/m
Primary suspension, vertical damper	1.1 E4	N s/m
Primary suspension, bush vertical stiffness	3.0 E6	N/m
Secondary suspension, longitudinal stiffness	2.57 E5	N/m
Secondary suspension, lateral stiffness	2.57 E5	N/m
Secondary suspension, vertical stiffness	2.55 E5	N/m
Secondary suspension, anti-yaw damper	Nonlinear, see Table 2	
Secondary suspension, lateral damper	3.7 E4	N s/m
Secondary suspension, bush lateral stiffness	3.0 E7	N/m

slightly higher than that of LMA and it is potential to increase the wheel tread conicity, as shown in Fig. 3.

The wheel tread conicity is considered as the indirect index of the dynamic behavior of the wheelset. The wheel tread conicity can be classified into three regions. The first one is related to the tread contact within 3-mm lateral displacement of wheelset. This region is responsible for motion on a straight track. The second region corresponds to 3~6-mm lateral displacement of wheelset, and this region is design to take effect of the curves with a large radius. The third one corresponds to the negotiation on sharp curve with the flange contact beyond 6-mm wheelset displacement.

In Fig. 3, it can be seen that the wheel tread conicity of LMD profile is much higher than that of LMA profile within 7-mm lateral displacement of wheelset. For the CRH1 train, the raising tread conicity in the region of 8–10-mm wheelset displacement can significantly increase the guiding force of the wheelset to improve the vehicle stability on straight track and curve line with a large radius. However, the transitional region of the LMD tread conicity from wheel tread to flange is not smooth enough as expected. In this manner, when a vehicle is passing the sharp curve, the guiding force of wheelset will be not enough within 9-mm wheelset displacement; then, the lateral displacement of wheelset should be increased exceeding 9 mm. In this case, the wheel flange will certainly contact with rail gauge corner to steer the wheelset and then cause wheel flange/rail gauge corner wear.

The contact points of the LMA and LMD wheel profiles on CN60 rail are shown in Fig. 4. The lines between the wheel

Table 2 Nonlinear characteristics of anti-yaw damping of the secondary suspension stage

Velocity (m/s)	0.01	0.04	0.1	0.2
Force (N)	4600	12,000	13,500	15,500

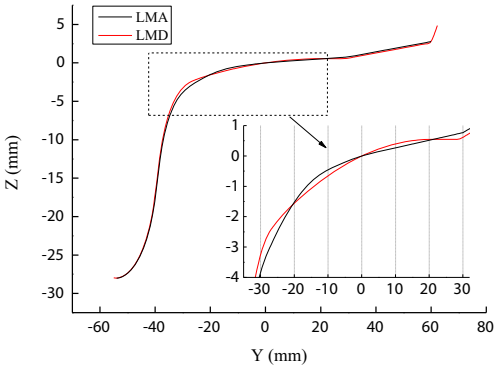

Fig. 2 Wheel profiles LMA and LMD

and rail represent the corresponding contact points and the value of corresponding lateral displacements of wheelset are shown in above the wheel profile. The contact points of LMD profile are more dispersed than that of LMA profile. Within 9-mm lateral displacement of wheelset, the contact points of LMD profile normally concentrate around the middle of the wheel tread. When a vehicle passes a sharp curve, the LMD profile is not able to provide enough guiding force in contact area, while the displacement of wheelset continuously keep increasing until the wheel flange meets the rail.

The results of dynamic simulations of the CRH1 vehicle with LMA and LMD wheel profiles are shown in Figs. 5, 6, 7, 8, 9, 10, and 11. The CRH1 train model was built in a multi-body dynamic software, SIMPACK. The critical speed of the vehicle with the two profiles is set to 374 km/h in LMA and 373 km/h in LMD, which are fast enough to meet the requirement of 200 km/h for the operation speed. The difference of the wheel geometry leads to different vehicle dynamic behaviors between LMA and LMD. Figure 5 shows the lateral acceleration of wheelset and car body when the vehicle running on a tangent line with measured rail irregularity in Chinese high-speed rail. In Fig. 5, it is clear that the lateral acceleration of wheelset and car body using LMD profile is much smaller than that of LMA profile. It is obvious that the LMD profile can slightly increase the stability of the CRH1 vehicle.

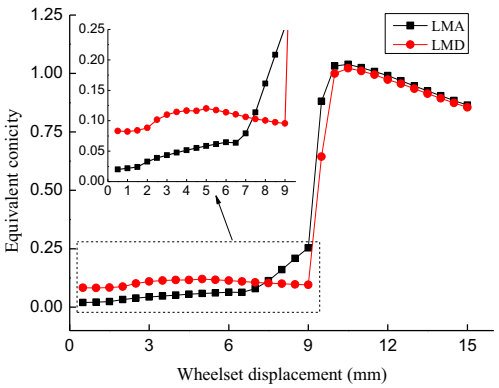

Fig. 3 Wheel tread conicities for LMA and LMD wheels on CN60 rail

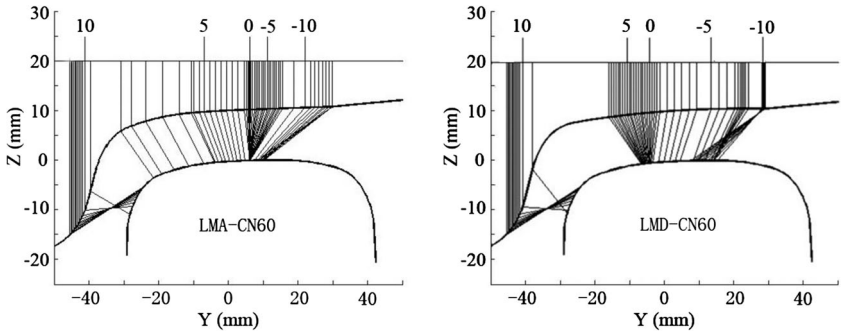

Fig. 4 Position of contact points on wheel and rail depending on lateral displacement of wheelset

The ride indexes of the vehicle at different speeds are simulated and calculated using Sperling's filter (Cui et al. 2010) as shown in Fig. 6. The lateral ride indexes of the vehicle with two different profiles can both increase with the speed increasing. However, the growth of LMD profile is slower than that of LMA profile. When the vehicle speed exceeds 140 km/h, the ride indexes of LMD profile start to provide smaller value than that of LMA profile, which means the LMD profile is sufficient to provide better ride comfort to the CRH1 vehicle on tangent track.

Most of the high-speed lines are composed of the tangent track or curved track with the radius greater than 6000 m. In recent study, a curved section which consists of 2000 m is used for a sample track in dynamic simulation. The first section of track line was designed with a tangent part of 320 m, a transition part of 200 m, a curved part of 1000 m, and a radius of 7000 m, and then extended by connecting to a transition part of 200 m and a straight part of 280 m in the rest of track line, as shown in Fig. 7 curve 1. The super elevation is 100 mm. Figure 7 gives the dynamic behavior when the CRH1 vehicle passing that track at a speed of 200 km/h. The vehicle using LMA wheels is unstable on transition part of the track. The lateral displacement of LMD wheelset is smaller than that of LMA wheelset on the curved track because the LMD has the larger wheel tread conicity which can provide larger guiding force.

The curving performance, when vehicle negotiates a narrow curve, is also simulated as shown in Fig. 9. The curve is set to relate to a realistic line in Shanghai as shown in Fig. 7 curve 2, 30-m tangent track, 40-m transition track, then a curved part of 100 m with a radius of 300 m, followed by 40-m transition line and 50-m straight line. There is no super elevation on this curve. The train running speed is set to 9 km/h. When the CRH1 vehicle negotiates on the narrow curve, the lateral displacements of the LMA and LMD wheelsets are both around 9.5 mm, which can cause the contact between wheel flange and the rail and result in significant wear of wheel flange/rail gauge corner. Actually, when a vehicle passes this curve, the large lateral displacements of wheelset and angle of attack can bring about two-point-contact (Cui et al. 2016). Additionally, the lateral force of LMD wheel is larger than that of LMA wheel as shown in Fig. 9b, which indicates that a larger wheel flange/rail gauge corner wear occurred by using LMD wheel.

3 Optimization problem definition

3.1 Design variables

In the study of the wheel optimization, the profile can normally be described in two ways. One derives some relationship to get the mathematical expression of the wheel profile (Wu 2000; Zhang et al. 2008; Shen and Zhong 2010), and the other applies the interpolating fitting curve to represent the wheel profile (Shevtsov et al. 2005; Markine et al. 2007; Jahed et al. 2008; Cui et al. 2011). In this study, 15 points on the profile have been selected between flange and filed side to represent

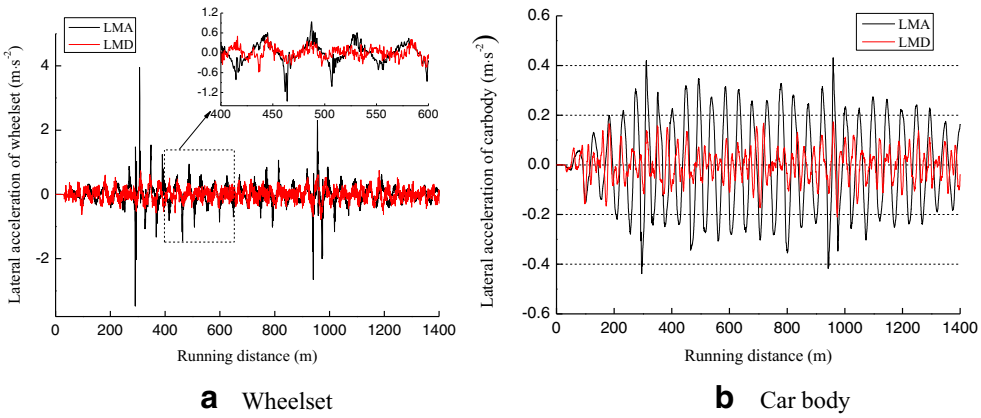

Fig. 5 The lateral acceleration

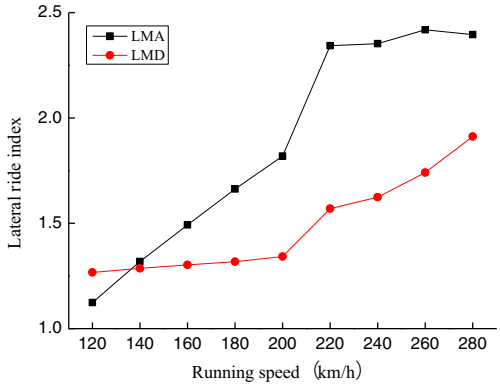

Fig. 6 Lateral ride index

the wheel profile as shown in Fig. 10. The nodes on the surface of the wheel profile express as the uniform distribution on the wheel profile from −40 to 30 mm. Point *A* is on the position of the rolling circle in name at coordinates of (0, 0). Point *B* is on the wheel flange and the lateral distance to point A is 40 mm. Points *A* and *B* have been fixed to ensure the profile have the same size of wheel flange and wheel diameter. The lateral coordinates of the moving nodes are set to be constant, and the vertical coordinates are considered as variable values. The wheel profile in the optimization region can be generated through fitting the constant and variable nodes by using cubic spline function. The original wheel flange curve can be directly connected to the optimization region, and a straight line which has the same slope as the last nodes *C* is also connected; then, a complete wheel profile can be created and expressed by the vertical coordinates z_0, z_1, …, z_{14} as $f(\mathbf{z})$. There, $\mathbf{z} = [z_1 z_2, \ldots, z_8, z_{10}, \ldots, z_{14}]$ is the design variable.

To ensure wheel flange and straight line smoothly, some boundary conditions are set at the start point *B* and end point *C* as follow

$$\begin{array}{lll} \text{Starting} & \text{slope}: & l_B = \tan(70) \\ \text{Ending} & \text{slope}: & l_C = 1/40 \end{array} \quad (1)$$

3.2 Objective function

Based on the above study and the actual operation of the CRH1 train, the LMA and LMD wheels both of them have advantages and disadvantages. In recent study, the main objective is to create an optimal wheel profile which can coordinate the trade-off between ride comfort (better in LMD profile) and wheel flange/rail gauge corner wear (less in LMA profile).

The most direct goal of wheel tread design is, of course, to achieve the optimal running stability and ride comfort of the vehicle and the lowest wear index of the flange and tread, but these parameters cannot be obtained at the same time. The dynamic behaviors of vehicle running on tangent or curved track are even contradictory. In addition, the relationship between these performance indexes and wheel profile cannot be directly established by mathematical expressions, but must be correlated with each other by numerical methods, which makes it difficult to establish objective functions and select optimization methods.

In order to simplify the calculation process, the lateral acceleration of the car body is selected to represent the ride comfort index in tangent track and large curved track, the lateral force of wheel and rail and angle of attack are chosen to indicate the wheel flange/rail gauge corner wear. Therefore, the target functions are written as

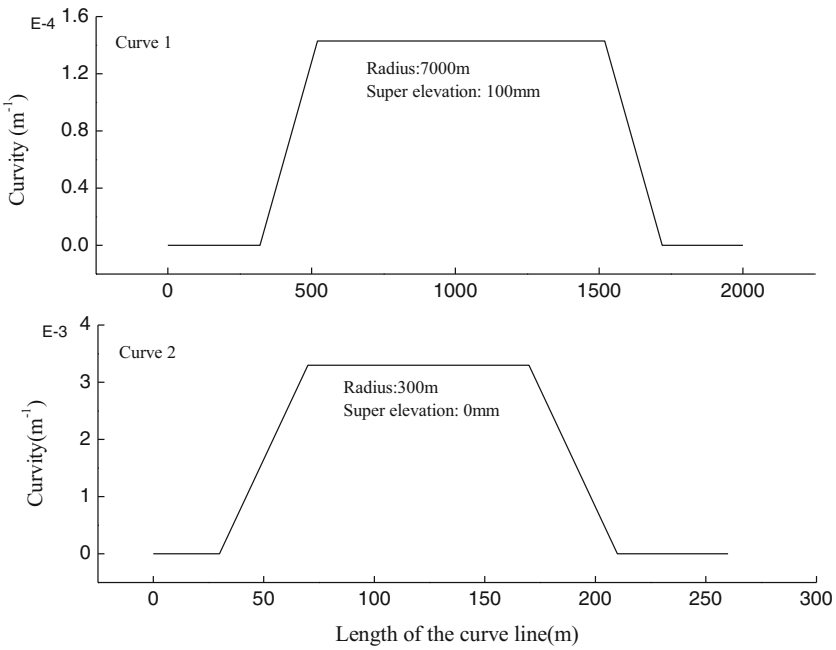

Fig. 7 Parameters of the curve lines

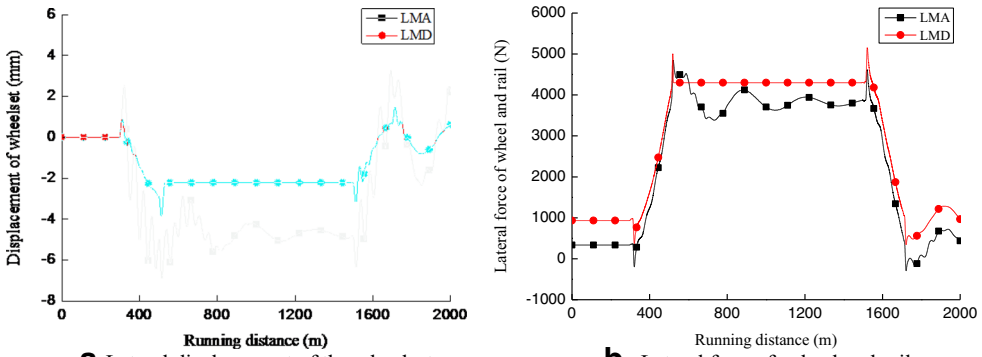

Fig. 8 Curve negotiation performance with large radius

a Lateral displacement of the wheelset **b** Lateral forceof wheel and rail

$$\text{Minimize}: \begin{cases} f_1(z) = \max(|Q_i|) \\ f_2(z) = \max\left(\left|Q_{i,j}\right|\right) \\ f_3(z) = \text{Rms}(A) \end{cases} \quad (i = 1,2,3,4; j = l,r) \tag{2}$$

where f_1 is the maximum angle of attack of the four wheelsets in the vehicle. φ_i is the angle of attack of the ith wheelset. f_2 is the maximum lateral force of j side wheel/rail on the ith wheelset. f_3 is the root mean square value of car body acceleration A. The measurement point of the acceleration is one of the marker points of air springs on the car body. The RMS value is calculated over 100-m distance with a step of 10 m.

In order to obtain an integrated objective function, the amplification coefficients are employed to change the values of the three targets to the same magnitude. In addition, the weighted factors are used to consider the importance of each objective. So the objective function can be written as

$$f(z) = 10,000w_1f_1 + w_2f_2 + 100w_3f_3 \tag{3}$$

3.3 Design constraints

The design variables must meet the requirement of the monotonicity of the wheel profile curve. Hence, the constraint equation is employed as

$$G_k = \frac{Z_k - Z_{k-1}}{y_k - Z_{k-1}} > 0, \quad k = 1,2,\ldots,14 \tag{4}$$

In optimization process, the vehicle dynamic behaviors are calculated to ensure the generate wheel profile meet the requirement of derailment security, denotes by

$$g_1 = \max\left(\left|\frac{Q_{i,j}}{P_{i,j}}\right|\right) < 1 \tag{5}$$

and

$$g_2 = \max\left(\left|\frac{P_{i,l} - P_{i,r}}{P_0}\right|\right) < 0.6 \tag{6}$$

In (5) and (6), P is the vertical force of wheel and rail. Q is the lateral force of wheel and rail. P_0 is half of the axle load.

4 Optimization algorithms

According to (1)–(9), the optimization method can be described by

$$\begin{aligned} &\text{Minimize}: f(z_0, z_2, \ldots, z_{14}) = f(\mathbf{z}), \mathbf{v} \in \mathbf{R}^N \\ &\text{Subject} \quad \text{to}: G_k > 0, g_1 < 1, g_2 < 0.6 \end{aligned} \tag{7}$$

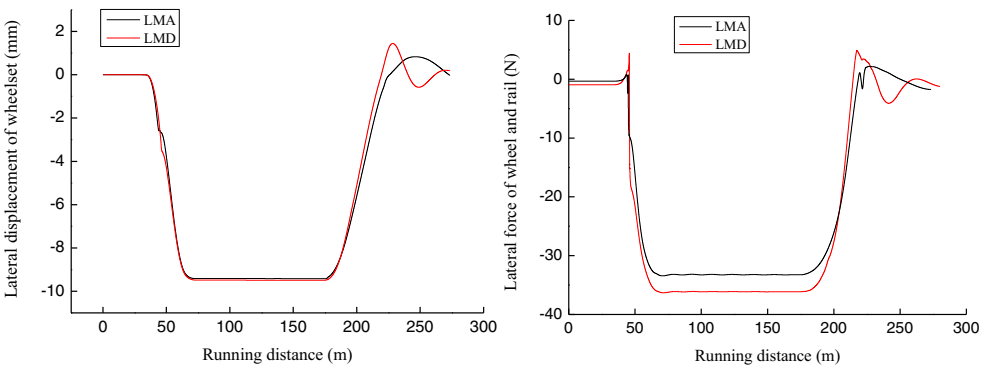

Fig. 9 Curve negotiation performance with narrow radius

a Lateral displacement of wheelset **b** Lateral force of wheel and rail

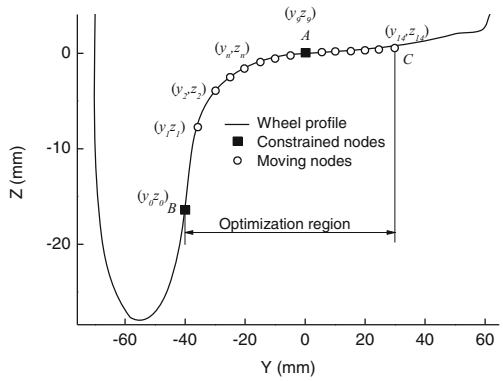

Fig. 10 The expression of the wheel profile

It is clear that all the functions of this method have no analytical expressions and can be obtained through Simpack computational package, and it can be seen as the limitation of using the conventional optimization method.

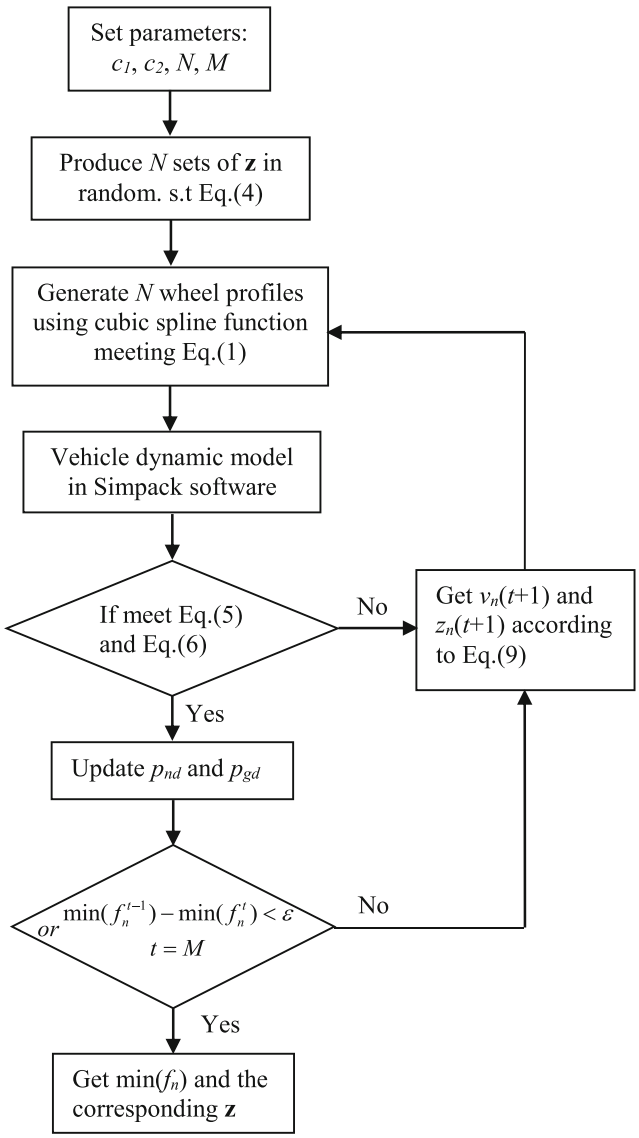

Fig. 11 The flow chart of optimization

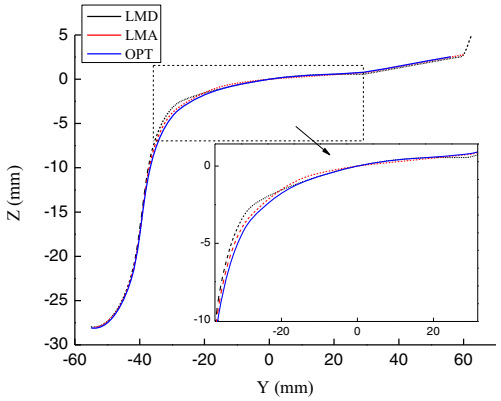

Fig. 12 Wheel profiles LMD, LMA, and OPT

In this section, the particle swarm optimization (PSO) (Clerc and Kennedy 2002; Ratnaweera and Halgamuge 2004) is used to solve the problem. In order to improve calculation efficiency and ensure the better convergence properties of the algorithm, the time-varying acceleration coefficients are given as

$$c_{1t} = \alpha\frac{M-t}{M} + c_1, c_{2t} = \alpha\frac{t}{M} + c_2 \tag{8}$$

where c_1, c_2, α, are constants. M is the maximum number of allowable iterations. t is the current iteration number. c_{1t} and c_{2t} are the current acceleration coefficients.

The iterative formula can be written as

$$\begin{aligned} \nu_{\mathrm{nd}}(t+1) &= \chi\left[\nu_{\mathrm{nd}}(t) + c_{1t}r_1(p_{\mathrm{nd}}(t) - x_{\mathrm{nd}}(t)) + c_{2t}r_2\left(p_{\mathrm{gd}}(t) - x_{\mathrm{nd}}(t)\right)\right] \\ z_{\mathrm{nd}}(t+1) &= z_{\mathrm{nd}}(t) + \nu_{\mathrm{nd}}(t+1) \end{aligned} \tag{9}$$

In (9), $n = 1, 2, \ldots, N$ and N is the number of the wheel profiles in an algorithm called population dimension. $d = 1, 2,$

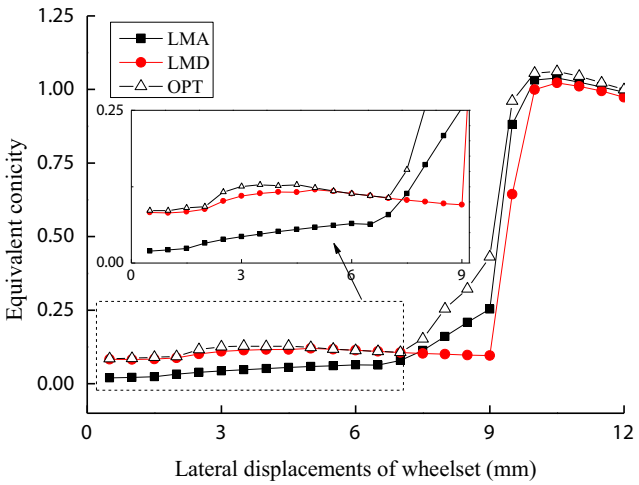

Fig. 13 Equivalent conicity of wheel profiles LMA, LMD, and OPT

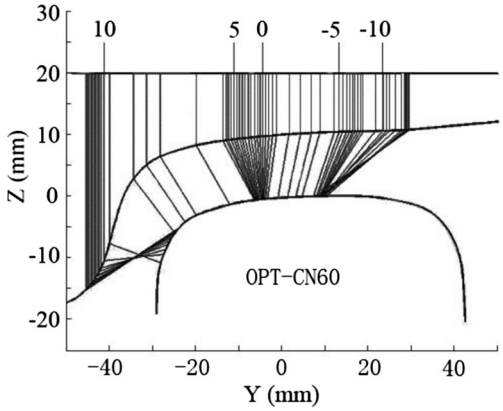

Fig. 14 Position of contact points on wheel and rail

…, D and D is the dimension of variables vector space. In this study, D = 13, v_{nd} is termed the velocity of each particle, according to its own flying experience and the flying experience of the other particles in the search space. z_{nd} is the position of each particle and the position of each particle is a potential solution. p_{nd} is the best position of each particle, and p_{gd} is the fittest particle found so far at the time t. r_1 and r_2 are the pseudo random number independent of each other and submit to a uniform distribution in [0, 1]. χ is the compress factor and expressed as

$$\chi = \frac{2}{\left|2-C-\sqrt{C^2-4C}\right|}, C = c_{1t} + c_{2t}, C > 4 \tag{10}$$

The typical structure of the PSO method using on a wheel profile optimization is shown in Fig. 11 In this study, $c_1 = 2.5$, $c_2 = 2$; $\alpha = 1.5$, $M = 150$, $N = 5$. The population dimension N and the maximum number of allowable iterations M dictates the computing time and accuracy. Of course, the parallel programs can be used to run Simpack model with N wheel profiles at the same time. There are 3 computing cases in Simpack, tangent track, large curved track and sharply curved track. The parameters of each case are set as chapter 2. The target function f_1 and f_2 are only related to the

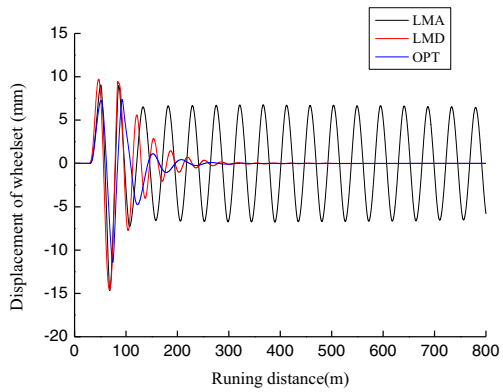

Fig. 15 Displacement of the wheelset

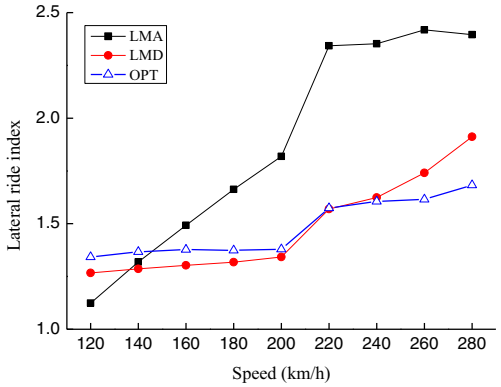

Fig. 16 Lateral ride index

sharply curved track, and f_3 is decided by tangent track and large curved track. Therefore, the weighted factors are set as $w_1 = w_2 = 0.3$ and $w_3 = 0.4$ based on experience.

In the optimization progress, the termination conditions are set as

$$\text{or} \min\left(f_n^{t-1}\right) - \min\left(f_n^t\right) < \varepsilon \quad t = M \tag{11}$$

where ε is the allowable tolerance.

5 Results and discussion

The optimization procedure is shown in Fig. 11 and has been implemented using MATLAB software. The first work in progress of optimization is to set the parameters, *c1*, *c2*, *N*, *M*, which were used in PSO method. Then N sets of **z** are produced in random and N wheel profiles are generated through connecting each sets of **z** using cubic spline function meeting (1). Send the profiles into vehicle dynamic model established in Simpack and do the simulation.

If the results meet (5) and (6), then update the parameters p_{nd} and p_{gd} and judgment of the termination conditions (11). If meeting (11), the optimization breaks and obtains the minimum value of $f(\mathbf{z})$ and the corresponding **z**. Then, the optimization profile can be obtained by connecting each point using cubic spline function-based **z**. If the results do not meet (5), (6), or (11), the v_n $(t+1)$ and z_n $(t+1)$ will be gotten according to (9) and other N wheel profiles will be generated. The whole optimization progress is in a close loop until an optimized profile is obtain.

The result OPT profile is shown in Fig. 12 compared with LMA and LMD profiles. The OPT profile has the similar shape with the LMA and LMD profiles close to the rolling circle in name, but also have a distinct difference on the flange root section in comparison to two previous profiles. This is because the LMD profile has an outstanding behavior on tangent track but it is not able to provide sufficient guide force on

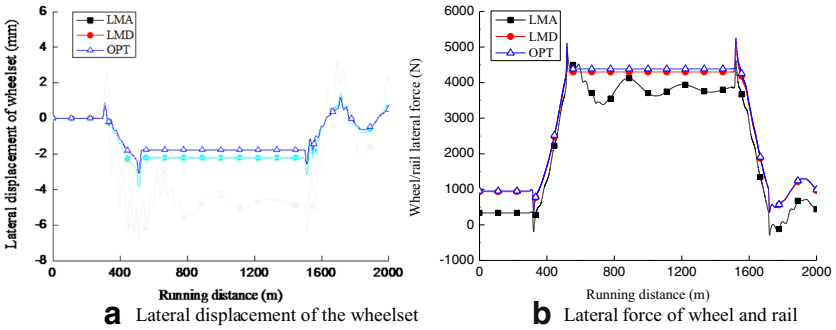

Fig. 17 Curve negotiation performance with large radius

a Lateral displacement of the wheelset **b** Lateral force of wheel and rail

a curved track. From Fig. 13, where the equivalent conicity is shown, it is evident that the OPT profile has the similar values of equivalent conicity within 7-mm wheelset later displacement which ensures the outstanding behavior of wheels on the tangent track. Meanwhile, the conicity in the range from 7 to 9 mm wheelset displacement increases gradually, which can provide a better curving performance compared with the conicity status of LMD profile in this zone.

The distribution of contact points versus lateral displacement of the wheelset was calculated and shown in Fig. 14. When the displacement of wheelset is beyond 7 mm, the contact points will pass through the wheel flange root gradually instead of jumping from wheel tread to the wheel flange as LMD profile. This contact characteristics have benefits for improving curving performance and reducing wheel flange wear.

Figure 15 shows the displacement of the wheelset when the vehicle runs on a tangent track and passes a lateral sinusoidal irregularity excitation at a speed of 300 km/h. It can be seen that the vehicle with LMA profile is instable when passing the irregularity excitation. The OPT and LMD profiles both can ensure the vehicle passing the excitation smoothly. According to the result of the simulation, the OPT profile can provide a higher critical speed of 396 km/h than using LMD profile. The lateral ride index of the vehicle with OPT profile is higher than LMD profile when the vehicle running speed is under 220 km/h. When the speed exceeds 220 km/h, the lateral ride index of OPT profile is reduce to be smaller than LMD profile as shown in Fig. 16.

The curve negotiation performance of OPT profile with radius of 7000 m was calculated and is shown in Fig. 17 compared with LMA and LMD profiles. It can be seen that the lateral displacement of the wheelset using OPT profile is the lowest one and the lateral force of wheel and rail is the highest in those three profiles due to the high conicity of OPT profile. When a vehicle passes the narrow radius curve, shown in Fig. 18, the lateral displacement of the wheelset on OPT profiles is obviously lower than the other profile, which can reduce the lateral force between wheel flange and rail gauge corner.

To compare the vehicle dynamic behavior of the three profiles, the curve negotiation performance with different radiuses was calculated as shown in Fig. 19. It can be seen that the lateral displacement of wheelset and wheel/rail lateral force is gradually increased with the curve radius decreases. When the curve radius is over 3000 m, the lateral displacement and force are changed slowly. Once the curve radius smaller than 3000 m, the wheel flange will contact the rail and lead to the lateral displacement of wheelset and wheel/rail lateral force increase rapidly. According to OPT profile can employ the root of the wheel flange to translate the contact point from wheel tread to wheel flange, the displacement and wheel/rail force becomes smaller than LMD profile at the same curve radius.

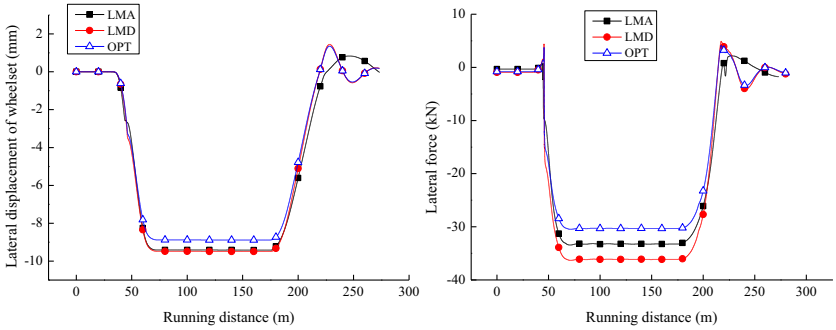

Fig. 18 Curve negotiation performance with narrow radius

a Lateral displacement of wheelset **b** Lateral force of wheel and rail

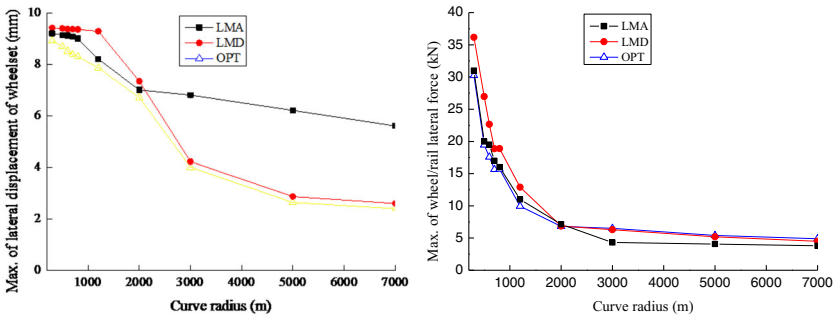

Fig. 19 Curve negotiation performance with different radiuses

6 Conclusions

In the present work, a comparative analysis of the performances of the LMA and LMD profiles on the CRH1 vehicle is given. Subsequently, a multi-objective optimization method is introduced for the design of wheel profiles to reduce the wheel flange/rail gauge corner wear on the premise of ensuring the dynamic behavior of the vehicle. A closed-loop program is completed in Matlab software, in which the particle swarm optimization method is employed for seeking the optimum profile and the vehicle dynamic behavior is obtained by Simpack.

The procedure is applied to the design of a new profile for the CRH1 train in China. Comparative results obtained from a behavior simulation show that the optimized profile can reduce wheel/rail lateral force in the sharply curved track without loss dynamic behavior in a tangent and large curved track.

This method is not limited to the objective function used here, but can easily be altered to add other criteria based on the problems that occur in practice. It can also be applied to design a rail profile to determine the amount of rail grinding.

However, the wear and instability of vehicle are not solely due to the wheel profiles; modification of wheel profiles is also not the simple means to solve these problems. To solve such complex problems, the factors affecting the wheel flange wear, vehicle dynamic behavior, and maintenance costs should be considered overall. Actually, simultaneous with the wheel profile optimization, track and vehicle parameter modification and implementation of lubrication measures were also taken into account in this project.

Funding information The present work has been supported by the National Natural Science Foundation of China (Nos. 51605394 and U1434210), the Department of Education Foundation of Sichuan Province (No. 16ZB0011), and the Key Research Project of Leshan City (No. 16ZDYJ0147).

References

Clerc M, Kennedy J (2002) The particle swarm-explosion, stability, and convergence in a multidimensional complex space. IEEE Trans Evol Comput 6(1):58–73

Cui D, Li L, Jin X, Li L (2010) Wheel-rail profiles matching design considering railway track parameters. Chin J Mech Eng 23(4): 410–417

Cui D, Li L, Jin X (2011) Optimal design of wheel profiles based on weighted wheel/rail gap. Wear 271:218–222

Cui D, Wang H, Li L, Jin X (2015) Optimal design of wheel profile for high-speed train. P I MECH ENG F-J RAI 229(3):248–261

Cui D, Zhang W, Tian G et al (2016) Designing the key parameters of EMU bogie to reduce side wear of rail. Wear 366-367:49–59

Haque I, Latimer DA, Law EH (1989) Computer-aided wheel profile design for railway vehicles. ASME J Eng Ind 111:288–291

Heumann H (1934) Zur Frage des Radreifen-umrisses. Organ Forts Eisenba 89(18):336–342

Ignesti M, Innocenti A, Marini L, Meli E, Rindi A, Toni P (2013) Wheel profile optimization on railway vehicles from the wear viewpoint. Int J Nonlin Mech 53:41–54

Jahed H, Farshi B, Eshraghi MA, Nasr A (2008) A numerical optimization technique for design of wheel profiles. Wear 264:1–10

Jin X, Shen Z (2001) Development of rolling contact mechanics of wheel/rail systems. Adv Mech 31(1):33–46

Liu X (2000) Development of arc-shaped tread contour for locomotives and rolling stock. Rolling Stock 38(2):24–28

Markine VL, Shevtsov IY, Esveld C (2007) An inverse shape design method for railway wheel profiles. Struct Multidiscip Optim 33: 243–253

Polach O (2011) Wheel profile design for target conicity and wide tread wear spreading. Wear 271:195–201

Ratnaweera A, Halgamuge S (2004) Self-organizing hierarchical particle swarm optimizer with time-varying acceleration coefficients. IEEE Trans Evol Comput 8(3):240–255

Sato E (2000) The scientific design of wheel tread shape. J Fore dies Locom 3:39–43

Sato Y (2005) History study on designing Japanese rail profiles. Wear 258(7–8):1064–1070

Shen G, Ayasse JB, Chollet H et al (2003) A unique design method for wheel profiles by considering the contact angle function. Proc IMechE F J Rail Rapid Transit 217:25–30

Shen G, Chollet H, Ye Z (2005) Study on wheel profile and contact analysis. J Chin Rai Soci 27(4):25–29

Shen G, Zhong X (2010) Inverse method for design of wheel profiles for railway vehicles. J Mech Eng 16:41–47

Shevtsov IY, Markine VL, Esveld C (2005) Optimal design of wheel profile for railway vehicles. Wear 258:1002–1030

Wickens AH (1998) Dynamics of railway vehicles - from Stephenson to Carter. Proc Inst Mech Eng F J Rail Rapid Transit 212(3):209–217

Wu H M. (2000). Investigations of wheel/rail interaction on wheel flange climb derailment and wheel/rail profile compatibility [D]. The Graduate College of the IIT

Yang G (1978a) A preliminary study of wheel tread shape (upper section)[J]. Rolling stock 11:1–6

Yang G (1978b) A preliminary study of wheel tread shape (lower section)[J]. Rolling stock 12:1–17

Zhang J, Wen Z, Sun L, Jin X (2008) Wheel profile design based on rail profile expansion method. Chin J Mech Eng 44(3): 44–49

Zhang S, Gu J (2009) Thinking and assumption of independent innovation of wheelset for high-speed cars in China. Rolling stock 47(3):1–5